Micro-scale Fixtures and Positioning Stage For Dual-Stage Hard Disk Drive Assembly

by

Sarah Felix

B.S. (Boston University) 2000

A thesis submitted in partial satisfaction
of the requirements for the degree of

Master of Science

in

Mechanical Engineering

in the

GRADUATE DIVISION

of the

UNIVERSITY OF CALIFORNIA, BERKELEY

Committee in charge:

Roberto Horowitz, Chair
Masayoshi Tomizuka

Spring 2007

The thesis of Sarah Felix is approved.

Chair	Date
	Date

University of California, Berkeley

Spring 2007

Micro-scale Fixtures and Positioning Stage For Dual-Stage Hard Disk Drive Assembly

by

Sarah Felix

Abstract

Micro-scale Fixtures and Positioning Stage For Dual-Stage Hard Disk Drive Assembly

by

Sarah Felix

Master of Science in Mechanical Engineering

University of California, Berkeley

Roberto Horowitz, Chair

Dual-stage servo technology has proven necessary in reaching 1 Tbit per square inch data densities in hard disk drives. One type of dual stage system, developed by the Computer Mechnics Laboratory at UC Berkeley, uses a MEMS electrostatic actuator situated between the tip of the suspension arm and the slider. Position and orientation of the slider impact the performance of the track-following servo. In addition, assembly quality is critical to the mechanical robustness of the system in an operating disk drive environment. A micro-scale silicon fixture was designed and fabricated to accurately and repeatably mount the slider onto the microactuator. A small scale positioning stage was built to aid in installation of the actuator-slider assembly onto the suspension. Finally, an auxiliary fixture was created to aid in wirebonding steps. The new assembly process significantly improved labor time, positioning accuracy, and mechanical robustness of the assembly. In addition to describing the design and fabrication processes, this report also provides step-by-step guidelines for the component assembly process.

Roberto Horowitz
Dissertation Committee Chair

To my family.

Contents

List of Figures

List of Tables

Acknowledgements

I would first like to thank Professor Horowitz for his advice and encouragement while working on the disk drive project. I owe a debt of gratitude to Kenn Oldham who spent countless hours training me in microfabrication processes, and mentoring me in general. I also thank Stanley Kon and Carolyn White for their additional guidance. I appreciate the generous support from the staff in the Mechanical Engineering Department and the Berkeley Microlab. Finally, I'd like to specially thank my sister Elizabeth for the inspiration to pursue an advanced degree.

Chapter 1

Introduction

Increasing areal data densities in hard disk drives continue to motivate the development of high performance servo schemes for track-following control. Among the emerging configurations are dual-stage servos which incorporate a smaller scale actuator onto the disk drive suspension in addition to the voice coil motor (VCM) (1). One type of dual stage system developed by the Computer Mechnics Laboratory at UC Berkeley, uses a MEMS electrostatic actuator situated between the tip of the suspension arm and the slider, as shown in Figure 1.1 (2). The advantage of this configuration is that actuation of the slider relative to the suspension can occur downstream of suspension vibration modes. The electrostatic actuator is a translational type that displaces the slider normal to the data track, to assist in compensating for off-track disturbances.

The quality of assembly of the micro-scale servo components impacts the performance of the servo system. The position and orientation of the slider and actuator must be accurate

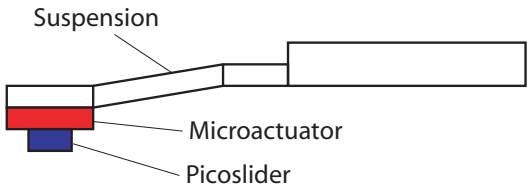

Figure 1.1. Side view schematic of disk drive suspension with MEMS actuator

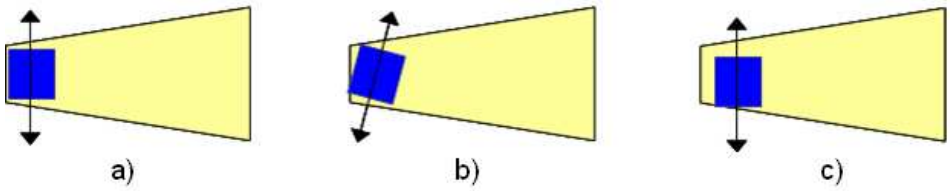

Figure 1.2. Assembly misalignment

and repeatable. If the slider-actuator assembly is angularly misaligned, as in Figure 1.2b, off-track motion is not maximized. If the slider is off center, as in Figure 1.2c, the bidirectional range of motion is not maximized and there will be bias in the microactuator displacement. Repeatability is important to minimize model error when designing the feedback system. Finally, reliable assembly techniques improve the mechanical robustness of the suspension assembly when subject to the operating disk environment.

Prior to the development of the assembly tools described in this paper, assembly of the slider, MEMS actuator and suspension components was done by hand. This resulted in excessive positioning error, handling damage and rework time. This paper describes the design, fabrication, and implementation of dedicated fixtures for the micro-scale assembly processes. In particular, bulk micromachining techniques are exploited to create a millimeter-scale silicon fixture with size tolerances on the order of one micrometer. Chapter 2 details the design and fabrication of this silicon fixture. Chapters 3 and 4 describe a positioning stage and wire bonding fixture that were also built to improve assembly. Chapter 5 discusses the implementation of the new assembly tools and resulting improvements. Chapter 6 contains conclusions and plans for future work.

Chapter 2

Microfixture Design and Fabrication

2.1 Silicon Fixture Design

2.1.1 Requirements

Figure 2.1 shows a drawing of the MEMS microactuator. Arrays of parallel plate capacitors (along the left and right sides of the drawing) provide translational motion when a voltage differential is applied. Secondary arrays of gap-closing capacitors (at the top and bottom of the drawing) provide on-board position sensing. Flexures provide the proper stiffness in different directions. The section in the center of the actuator is the shuttle, where the pico slider is mounted, as shown in the photograph in Figure 2.2.

The assembly fixture must meet several functional and geometric requirements. Most importantly, the pico slider must be centered on the shuttle with minimal misalignment. To achieve this, the fixture should have some edges or "datums" that seat the microactuator and other edges that locate the pico slider with respect to the actuator. Once these two components have been attached, the fixture must have yet another set of features to locate the microactuator-slider assembly with respect to the disk drive suspension tip.

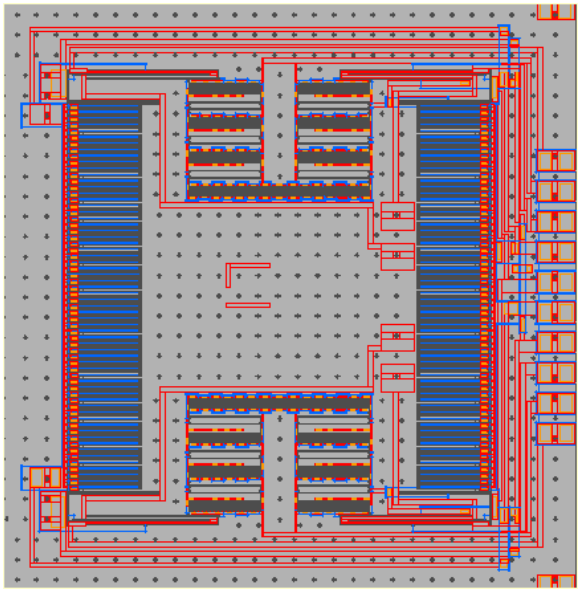

Figure 2.1. CAD drawing of MEMS actuator

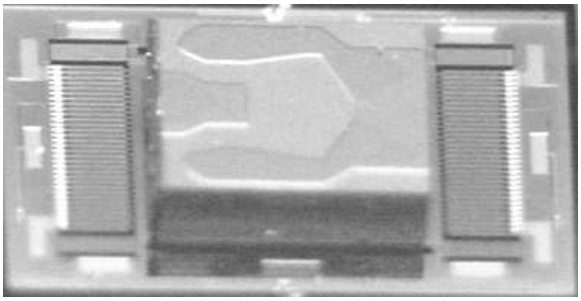

Figure 2.2. Photograph of pico slider mounted on microactuator

2.1.2 Concept Design

A silicon fixture built using microfabrication processes was selected because the locating features described above can have relative dimensions with tolerances on the order of micrometers. With such a fixture, several steps can be created in the silicon, each of which seats a different component, as illustrated in Figure 2.3.

As for the detailed configuration, several options were considered. The first is a simple square-window design illustrated in Figure 2.4a, where the microactuator would fit into one window and the slider would fit into another. The problem with this design is that it is difficult to manipulate the components if they are surrounded on all sides. Further, the

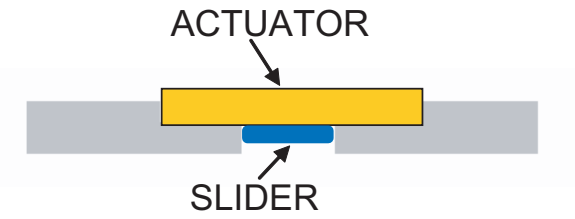

Figure 2.3. Cross-section of steps in assembly fixture

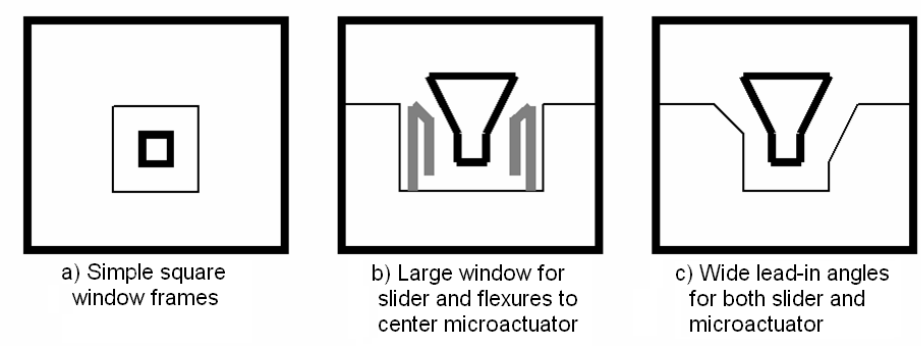

Figure 2.4. Sketches of fixture concepts considered

microactuator would not necessarily fit snugly in the window due to dimensional variations. Another concept, illustrated in 2.4b, has one open side and incorporates flexures to center the microactuator and hold it in place. The problem with this design is that the flexures would be difficult to fabricate, would be prone to breaking, and would not ensure perfect centering due to dimensional variations. In the chosen design, illustrated in 2.4c, the windows for each component are open on several sides and tapers are incorporated to guide the components into place with minimal damage. Two longer contact edges are retained for alignment of each component. Once butted against these edges, the microactuator can be secured with a temporary adhesive, such as photoresist. One additional modification required to this design is a cutout to make space for flash remaining from broken tethers at the bottom edge of the microactuator.

Visual alignment marks were chosen to address the alignment of the microactuator-slider assembly with respect to the suspension. Visual alignment is commonly used in microfabrication for such processes as lithography. Figure 2.5 shows a drawing of a typical suspension. The microactuator is mounted on the gimbal. The general process would be to

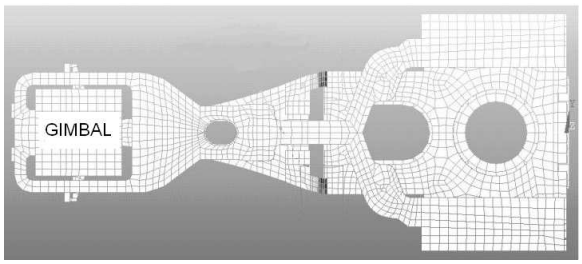

Figure 2.5. Hard disk drive suspension

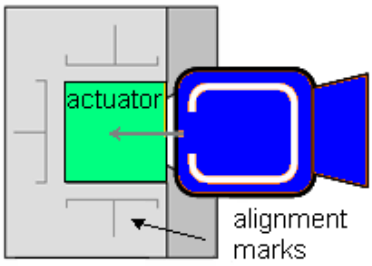

Figure 2.6. Schematic drawing of alignment of suspension over microactuator

lowered the suspension onto the back side of the microactuator while the microactuator is sitting in the fixture. This means that the microactuator would not be visible. Fortunately, the gimbal section is nominally the same size as the microactuator and has straight defined edges, providing a convenient feature for visual alignment. If the microactuator is secured in the fixture, visually aligning the suspension to the alignment marks on the fixture will ensure that the suspension is also aligned to the microactuator. This concept is illustrated in Figure 2.6.

2.1.3 Tolerances and Sizing Calculations

With the step design, the height of each step is important for proper function of the fixture. The picoslider should be below flush to avoid damage. The microactuator, on the other hand, should be above flush to allow contact with the suspension.

Nominal dimensions and estimated tolerances are given in Table 2.1.3. Thickness tolerances on silicon wafers can vary from $.5\mu m$ to 50 μm, depending on the quality specifications (3). A conservative tolerance of $25\mu m$ was assumed for step height thickness calculations. Etch depth tolerance was assumed to be +/- $5\mu m$ (this will be further justified in the fabrication section). Tolerances of the nitride and doped polysilicon layers on the microactuator are neglected compared to the other tolerances since they are both grown using highly controlled furnace processes. The step height d_{step}, is then

$$d_{step} = t_{MA,min} - dtol_e - 2.5\mu m = 90\mu m \tag{2.1}$$

		Nominal Dimension	Tolerance (+/-)
Slider height, t_s		.3 mm	.05 mm
Si Wafer thickness, t_w		500 μm	25 μm
Microactator total thickness, t_{MA}		102.75 μm	5.25 μm
	device layer	100	5 μm
	interconnects	1.25 μm	.25 μm
	nitride	0.5	neglect
	doped poly	1	neglect
Etch Depth tolerance, $dtol_e$		varies	5 μm

Table 2.1. Dimensions and tolerances for step height calculations

This ensures that the microactuator is at least $2.5\mu m$ above the surface. The minimum amount that the slider will lie below the surface, d_p is then

$$d_p = t_{w,min} - d_{step} - dtol_e - t_{s,max} = 30\mu m \tag{2.2}$$

A different approach was taken for the sizing of other dimensions on the fixture. Detailed tolerance information would be required to predict fit and interference issues. In particular, there should be adequate clearance for components in the windows, and the suspension should not obscure the visual alignment marks. However, because microfabrication enables fabrication of many devices on one wafer, several versions of the fixure were created with different dimensions to allow for dimensional variations.

2.2 Fixture Fabrication

2.2.1 Process Overview

Figure 2.7 illustrates the process sequence for the fabrication of the silicon fixture. The millimeter scale of the features is actually quite large for micromachining processes, so special considerations were made for large etch areas and step heights.

Since it is difficult to spin a quality layer of photoresist over a large step, a clever masking and etching sequence was implemented. Thick photoresist was used as a mask for

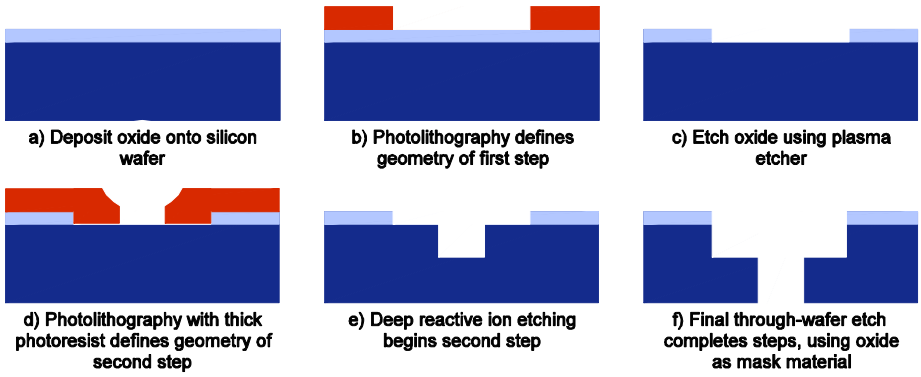

Figure 2.7. Process flow for silicon microfixture fabrication

etching the inner step and an oxide mask was used for etching the outer step. The oxide mask was patterned first on the bare silicon wafer using standard lithography and an oxide plasma etching system (Figure 2.7a-c). Then, thick photoresist was patterned for etching of the inner step (Figure 2.7d). Note that since the oxide layer is relatively thin, it did not present a problem when spinning on the thick photoresist.

The inner step was then etched using deep reactive ion etching (DRIE) (Figure 2.7e). The exact depth was not critical for this step, since this feature would ultimately be etched through the entire wafer. Once the thick photoresist was removed, the oxide mask was in place for the second DRIE step (Figure 2.7f). The thickness of this step was monitored more closely, since the depth is an important dimension, as calculated in the previous section. The etch rate of the process was about 2 $\mu m/min$, with variations across the wafer, leading to the estimated depth tolerance of about 5 μm. Table 2.2.1 summarizes the parameters for the masking materials, with selectivities and etch rates from (4).

Etch step	1 Inner Step	2 Outer Step
Etch depth	420μm	90μm
Etch rate	2 $\mu m/min$	2 $\mu m/min$
Etch time	210 min	45 min
Mask material	thick PR	oxide
Selectivity	100:1	100:1
Required mask thickness	4.2 μm	.9 μm
Actual mask thickness	9μm	1μm

Table 2.2. Etch depths, selectivities, and masking material thicknesses

Since the second etch step etched through the entire wafer, it was necessary to prepare a handle wafer on which to mount the process wafer. This was done by following the standard process outlined in (5). Table 2.2.1 lists the steps for the entire fabrication process along with the Microlab equipment used.

AutoCAD was used to generate the mask files for the two lithography steps, followed by several file conversions that are necessary for mask creation in the Berkeley Microlab.

2.2.2 Process Errors

Some rotational misalignment was introduced in the second lithography step because it was difficult to find some of the mask alignment marks on certain sections of the wafer. The worst case misalignment was visually estimated to be 3 μm. In addition, dimensional errors were introduced from using thick photoresist, which can limit feature resolution to 4 μm. Finally, during deep etching, side walls do not remain perpendicular throughout the depth of the etch, so there will be some edge location error on the order of 2 μm. Therefore, it was estimated that features on certain parts of the wafer could be misaligned up to about 10 μm.

Step	Equipment Used
1 Pre-Furnace Clean	Sinks
2 Wet Oxidation	Tystar Furnace
3 Prime wafers	HMDS Bubbler
4 Spin Photoresist	SVG Coater
5 Expose Wafers	Karl Suss Aligner
6 Develop	SVG Developer
7 Descum	Technics-C plasma etcher
8 Etch Oxide	LAM2 Oxide Autoetcher
9 Strip photoresist	PRS 3000 tank
10 Spin thick resist	SVG Coater
11 Expose Wafers	Karl Suss Aligner
12 Develop	SVG Developer
13 Hardbake	Small Oven
14 Descum	Technics-c
15 Bulk Etch 1	STS Reactive Ion Etcher
16 Remove PR	PRS3000 Tank
17 Prepare handle wafer	various
18 Bulk Etch 2	STS Reactive Ion Ethcer
19 Dice	Disco Dicing Saw

Table 2.3. Fabrication process

Chapter 3

Positioning Stage

The previous section described visual alignment marks that would be used for locating the suspension relative to the microactuator. For these micro-scale alignment marks to be effective, it is necessary to be able to manipulate the suspension very precisely. Ideally, the suspension should be manipulated in four axes: x, y and θ in the plane of the microactuator surface, and z for lowering the suspension to contact the microactuator after alignment.

Several options were considered for positioning of the suspension. One possibility would be to use existing positioning devices on equipment in the Berkeley Microlab, such as the probe station. The difficulty with this is that the manipulators would need to be adapted to hold the suspension. In addition, the prob station manipulators can only move objects precisely in the x, y, and z directions. The θ motion would be obtained by rotating the stage by hand, which would not be very precise. Instead, a custom positioning stage was designed and built using some salvaged parts from an optical experimental set up.

A photograph of the completed positioning stage is shown in Figure 3.1. Two translational micrometer-actuated positioning stages were stacked to achieve fine tuned x and y positioning. The suspension is fixed to this platform, and hovers over a second platform that holds the fixture with the microactuator-slider assembly. The second platform is rotated around its own vertical axis with another micrometer to achieve θ positioning.

The z positioning is less sophisticated. The suspension is bent at its hinge as depicted

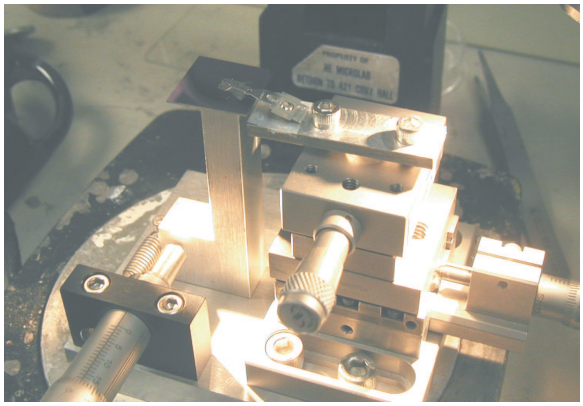

Figure 3.1. 3-axis micrometer positioning stage holding a suspension over a microactuator in the silicon fixture

in the side view in Figure 1.1. Therefore, a small shim is used to hold up the suspension and ensure the surface contacting the microactuator is horizontal. The shim and suspension are mounted on a plate with compliant spacers underneath and held in place by screws. The screws are used to adjust the horizontal position of the plate and lower the suspension.

One important consideration in designing the positioning stage was the overall height and footprint of the device. The entire setup had to fit underneath a microscope available in the Berkeley Microlab. This constraint motivated many of the dimensions of the positioning stage components. The entire stage is about three inches tall, with base dimensions 3 1/2" X 3".

Chapter 4

Wire Bonding Fixture

After the pico slider, microactuator, and suspension have been assembled, wire bonding is performed to connect the electrical leads on the suspension to the corresponding pads on the microactuator. Figure 4.1 shows wires bonded to the microactuator. This is a delicate procedure requiring proper support and protection of the components. Figure 4.2 highlights the areas that are supported during wire bonding. There must be solid support directly under the area of wiring to balance the contact forces of the wire bonder. There are other points at the base of the suspension head that are also supported. However, there are several features that protrude below the level of the supported surfaces that must not be damaged.

Supports were previously constructed from several small makeshift silicon shims placed

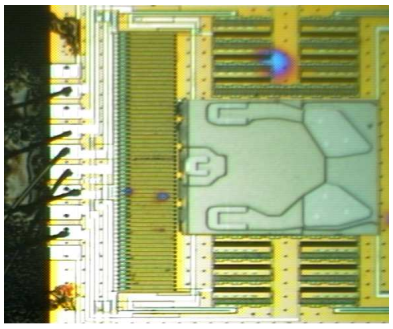

Figure 4.1. Wires (left) bonded to microactuator

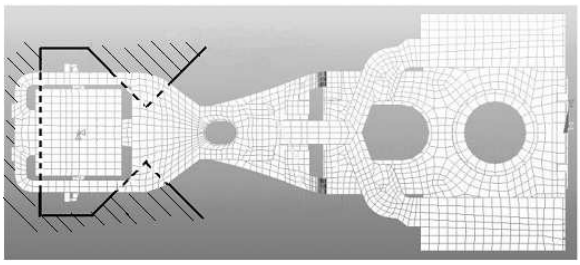

Figure 4.2. Drawing of suspension showing wire bonding fixture edges

Figure 4.3. Completed wire bonding fixture (left)

under the appropriate areas. This tended to be a bit sloppy and led to unnecessary damage and time spent on an already time intensive process.

An easy solution was to construct pre-built supports out of silicon using the same bulk micromachining processes used to create the assembly fixture. In fact, there was enough room on the silicon wafer used to make the assembly fixtures that the wire bonding support fixtures could be added at no additional cost. Figure 4.3 shows a completed wire bonding support fixture next to an actual suspension.

Chapter 5

Implementation

5.1 Assembly Process

A schematic of the assembly process is depicted in Figure 5.1. The following is the step-by-step procedure for component assembly using the assembly tools.

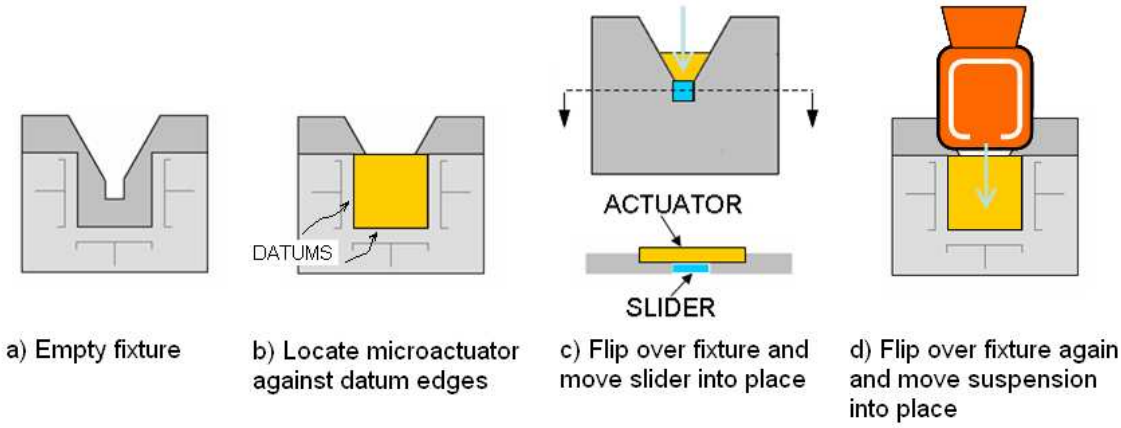

Figure 5.1. Assembly process flow

1. The microactuator is carefully placed in the silicon fixture and butted up against the two datum edges. Then, it is secured in place with a small drop of photoresist or other temporary adhesive that can be later dissolved. (Figure 5.1b and Figure 5.2)

2. After the adhesive dries, the fixture is flipped over to prepare for attachment of the

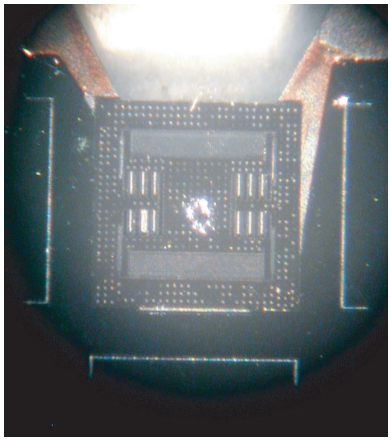

Figure 5.2. MEMS actuator seated in silicon fixture

Figure 5.3. Slider located and mounted on microactuator using silicon fixture

slider. Note that while the microactuator does protrude from the bottom of the fixture, it is the less-vulnerable backside surface that is exposed. (Figure 5.1c)

3. Next a small dot of epoxy is applied to the microactuator in the window where the picoslider is to be placed (the shuttle). Note that since the picoslider will be slid into position from the open side, the dot of adhesive should be placed closer to this open side. That way, it will be spread across the shuttle. (Figure 5.1c and Figure 5.3)

4. Allow sufficient time for the epoxy to dry.

5. Flip over the entire assembly fixture with the microactuator and slider. Mount fixture onto the rotational platform of the positioning stage using temporary adhesive or two-sided tape. The backside of the microactuator should now be facing upward. Mount the suspension on the translational platform of the positioning stage.

6. Apply a dot of epoxy onto the microactuator backside. Then, using the micrometer positioning stages, locate the suspension over the microactuator using the visual alignment marks. (Figure 5.1d and Figure 5.4)

7. Once in position, gently lower the suspension onto the microactuator. Leave components in position while the epoxy dries.

8. Remove the temporary adhesives to release the components from the fixture and positioning stage.

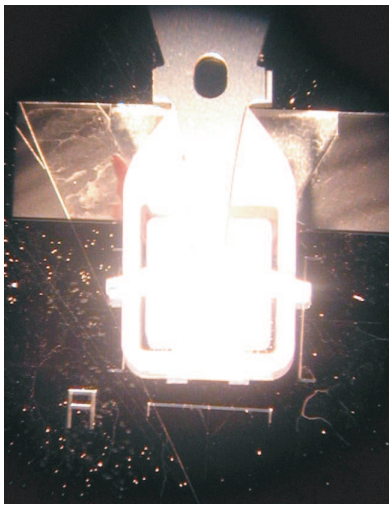

Figure 5.4. Suspension located over microactuator using visual alignment marks

9. Secure suspension assembly in wire bonding fixture using photoresist or other temporary adhesive.

5.2 Improvements

The assembly fixture significantly improved the step when the pico slider is attached to the microactuator. Out of all the dimensional variations of the fixture that were fabricated on the wafer, the version based on nominal dimensions worked best. The microactuator fit snugly, but with just enough clearance to slide in and out of the slot. The fixture not only reliably located the slider, but it protected the microactuator topside and capacitor arrays from handling damage. In addition much less adhesive is used, since the positioning of the slider is more precise and predictable. It is estimated that the slider can now be positioned to within +/- 5 μm.

The entire positioning stage fit under the available microscope and was thus easily integrated into the assembly process. The stage provided a more accurate and steady way to manipulate the suspension with respect the other components. Also during this step, the silicon assembly fixture provided support and protection for the slider that had been mounted on the microactuator.

The wire bonding fixtures were effective in providing support for the suspension during the wire bonding step.

5.3 Problems

The positioning stage was not as precise when lowering the suspension onto the microactuator. The simplistic platform with screws did not provide smooth, accurate manipulation in the z direction. An alternative mechanism for z axis positioning should be designed. This may be challenging due to the space constraints under the microscope that was used for assembly.

One problem that was not anticipated is that the silicon fixture eroded after multiple usages. This problem may be addressed by growing an additional film on the surface consisting of a harder material, such as nitride. However, this would complicate the fabrication process, change the fixture dimensions, and add undo cost to the devices. It is more feasible to just make replacement fixtures.

5.4 Performance Evaluation

Microactuators were installed into actual disk drives using the fixtures and techniques described in this paper. Figure 5.5 shows a schematic illustration of the experimental setup. Displacement measurements are made using a laser doppler velocimeter (LDV). Experimental transfer functions were measured from the VCM input to the slider displacement and from the microactuator input to the slider displacement. Figure 5.6 shows these experimental frequency responses. It can be seen that the microactuator is functioning properly and the transfer functions are fairly clean in the region around the microactuator resonance peak. Note that the low frequency spikes are the result of problems with the LDV measurements.

It was difficult to quantify the improvements in performance that resulted from the use of assembly fixtures. The suspensions used after the new assembly tools were implemented

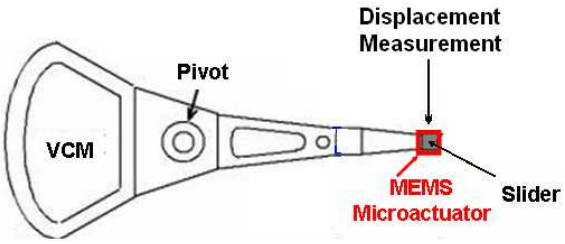

Figure 5.5. Schematic of experimental setup

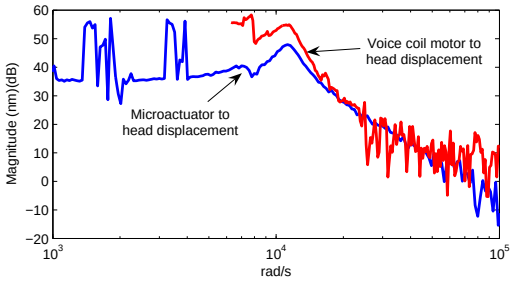

Figure 5.6. Experimental frequency response of disk drive with microactuator installed using assembly fixtures

had a different geometry than the previously used suspensions. However, for a rough comparison, microactuator transfer functions were examined for drives built before and after the implementation of the new assembly tools. Figure 5.7 shows frequency responses from two different drives built without the new assembly tools. Figure 5.8 shows similar frequency responses in drives built using the new assembly tools. The transfer functions in Figure 5.8 appear more consistant. However, due to the variation in suspension geometry, other inconsistent factors and the small number of trials, it is difficult to conclude whether or not this is due to improved assembly processes.

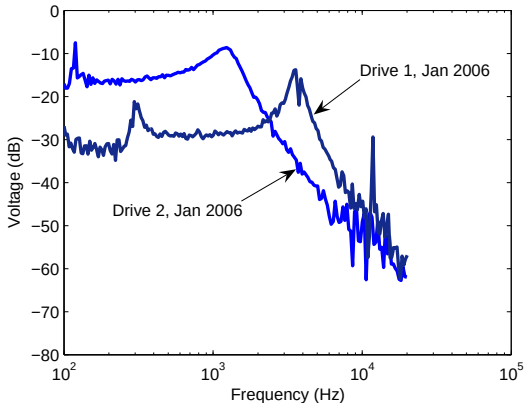

Figure 5.7. Experimental frequency response of two drives assembled without fixtures

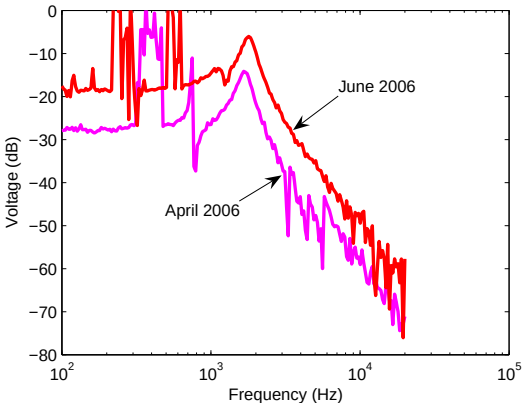

Figure 5.8. Experimental frequency response of two drives assembled with fixtures

Chapter 6

Conclusions and Future Work

The assembly tools described in this paper provided dramatic improvements in an assembly process that had been previously plagued by component damage and rework time. In particular, the assembly fixture enhanced positioning accuracy and repeatability of the slider on the microactuator. It also improved the ease and cleanliness of this assembly step. The wire bonding support fixtures provided proper support for the wire bonding process. Both the assembly fixtures and wire bonding fixtures represent a unique application of silicon bulk micromachining to create millimeter-scale tools with micrometer-scale dimensional accuracies.

The custom built positioning stage provided an effective means of manipulating the suspension with respect to the other components. However, the method of supporting the suspension and lowering it onto the other components was a too simplistic and required some tweaking. In the future, improvements should be made to modify the positioning stage for more reliable manipulation of the suspension.

While many of the improvements were qualitative and obviously worthwhile, it would be insightful to more rigorously quantify the performance improvements resulting from the use of assembly tools. This could be evaluated by examining experimental transfer functions of installed suspensions assembled with and without assembly tools. Identifying gain and natural frequency would yield insight about how the lateral range and modal dynamics are

affected. It would be expected that lateral range would on average be larger and modal dynamics would be more consistent. However, such a study could only be meaningful with an appropriate number of assembled plants, with negligible effects from other factors.

Bibliography

[1] R. Horowitz, T.L. Chen, K. Oldham and Y. Li, "Design, Fabrication and Control of Micro-Actuators for Dual-Stage Servo Systems in Magnetic Disk Files," *Springer Handbook of Nanotechnology*, ed. B. Bushan, Springer, New York, January 2004.

[2] K. Oldham, "Microdevices for Vibration Suppression in Computer Hard Disk Drives," PhD dissertation, University of California, Berkeley, 2006.

[3] Compart Technology Ltd., www.compart-tech.co.uk.

[4] M. Wasilik et al,"STS Poly/ Si Etcher," Berkeley Microlab Manual, 2006, http://microlab.berkeley.edu/labmanual/chap7/7.8.html.

[5] N. Chen, M. Wasilik, "MOD 35: Handle Bonding", Berkeley Microlab Process Modules, 2005 http://microlab.berkeley.edu/labmanual/chap1/1.3.html.